Journal of Crystal Growth 318 (2011) 995–999

Contents lists available at ScienceDirect

Journal of Crystal Growth

journal homepage: www.elsevier.com/locate/jcrysgro

Challenges in the crystal growth of Li_2CuO_2 and $LiMnPO_4$

Nadja Wizent [a,b,*], Günter Behr [a], Wolfgang Löser [a], Bernd Büchner [a], Rüdiger Klingeler [b]

[a] *IFW Dresden, Leibniz Institute for Solid State and Materials Research, 01171 Dresden, Germany*
[b] *Kirchhoff-Institut für Physik, Universität Heidelberg, Heidelberg, Germany*

ARTICLE INFO

Available online 2 November 2010

Keywords:
A2. Floating zone technique
B1. Lithium compounds
B1. Phosphates

ABSTRACT

Single crystals of a potential battery material, $LiMnPO_4$, and the spin ladder compound Li_2CuO_2 are grown under elevated gas pressure in a newly designed vertical floating zone facility with optical heating. Lithium vaporization and its reaction with gases in the growth chamber are principal challenges of the growth process. By applying high argon pressure of 40 bar during Travelling Solvent Floating Zone growth of $LiMnPO_4$ the vaporization was reduced by orders of magnitude. The optical radiation, penetrating the transparent melt, affects the crystal/melt interface curvature during the growth. The growth direction was recognized to be decisive for changing the interface curvature from concave to convex and enabling efficient grain selection. By using an Ar/O_2 gas mixture in crystal growth of Li_2CuO_2 the direct exchange between oxygen in the atmosphere and the floating zone, the oxygen content of the melt and finally the quality of Li_2CuO_2 crystals are controlled.

1. Introduction

Single crystals of large size are necessary to investigate the intrinsic properties of different types of materials. It is known that the use of high pressure of oxygen during growth can change the phase diagram and therefore the melting/crystallizing behaviour of oxide materials [1,2]. By using elevated argon pressure the vaporization of volatile elements can be reduced or avoided. These possibilities as well as the usage of gas mixtures with high pressure provide new prospects for crystal growth.

Crystals of two Li-compounds, the spin ladder compound Li_2CuO_2 and a potential Li-battery material $LiMnPO_4$, are prepared for the neutron scattering experiments and measurements of electric properties, respectively.

Both compounds are grown in a newly designed vertical floating zone facility with optical heating, which can be used with elevated gas pressure up to 150 bar.

$LiMnPO_4$ belongs to a family of potential cathode materials for Li-ion batteries, $LiMPO_4$ (M = Co, Fe, Mn and Ni). At present they are the most efficient energy storage systems. Till now most investigations have been done on polycrystalline powder and crystals grown by a flux method [3], but for studying their different properties—especially the anisotropic ones—single crystals of reasonable size are essential. 2005 first single crystals of $LiFePO_4$ were grown by the FZ method under an argon flow by Chen et al. [4]. Recently only bulk $LiCoPO_4$ single crystals were grown by an optical floating zone technique [5]. Saint-Martin and Franger mention serious vaporization during the growth. In this work we describe the growth of $LiMnPO_4$ under high pressure. By this we could avoid the vaporization of lithium oxide.

Li_2CuO_2 is the first [6] and the most frequently studied compound of the class of edge-shared spin-chain cuprates [7–9]. Owing to its structural simplicity with ideally planar CuO_2 chains it has been considered as a model quasi-one-dimensional (1D) frustrated quantum spin system.

2. Experimental

For both materials the feed rods were prepared by pestling the initial powders followed by a sintering procedure.

For $LiMnPO_4$ different powder preparation routes, which are described elsewhere [10], were examined to obtain a single phase compound material. Consequentially, the feed rods for floating zone experiments were made from the initial powders of Li_3PO_4 (Chempur 99+%), $MnCO_3$ (Aldrich 99.9+%) and $NH_4H_2PO_4$ (Chempur 99+%) in nominal molar ratios corresponding to stoichiometric $LiMnPO_4$.

The powder for the feed rods of Li_2CuO_2 was prepared by grinding and sintering LiOH (Isotec) and CuO (Chempur 99.99%) at 750 °C. To get high intensity for the neutron experiments special 99.9% ^{7}LiOH powder was used. Because the powder was single phase after the first sintering no further annealing was done to avoid additional vaporization of lithium.

---

* Corresponding author at: Leibniz-Institut für Festkörper und Werkstoffforschung (IFW) Dresden, Postfach 270116, D-01171 Dresden, Germany.
Tel./fax: +49 351 4659 562.
E-mail addresses: N.Wizent@ifw-Dresden.de, n.wizent@kip.uni-heidelberg.de (N. Wizent).

0022-0248/$ - see front matter © 2010 Elsevier B.V. All rights reserved.
doi:10.1016/j.jcrysgro.2010.10.029

The single phase powder has been pressed to polycrystalline rods (EPSI Engineered Pressure Systems; 3500 bar) in latex tubes with a diameter of 6 mm and sintered again at 800 °C for 34 h.

All crystals were grown in a vertical Travelling Solvent Floating Zone (TSFZ) facility with optical heating. The light of a 5 kW xenon arc lamp in the bottom of the facility is reflected on two ellipsoid mirrors and focussed in the crystal growth chamber. A cylinder only 72 mm long with 72 mm outer diameter and 14 mm wall thickness made of sapphire single crystal enables the use of up to 150 bar pressure of argon, oxygen or a gas mixture in the growth chamber.

During the growth process the temperature of the floating zone was measured with a two-colour pyrometer using a novel stroboscopic method [11]. By changing the pyrometer position also temperature gradients on the feed rod and crystal can be measured.

To study the melting behaviour of $LiMnPO_4$, Differential Thermoanalyses (DTA) were performed. Phase transformations and melting behaviour of selected samples were revealed on isochronal heating with 20 K/min up to a maximum temperature of 1095 °C in alumina crucibles within a SETARAM 92-24 high-temperature DTA device under flowing Ar.

The microstructures and crystal perfection of samples were investigated by optical metallography in polarized light and scanning electron microscopy (SEM). The compositions of phase constituents of polycrystalline samples and of grown crystals were determined by electron probe microanalysis (EPMA) applying the EDX mode. X-ray powder diffraction data were obtained by a Rigaku X-ray diffractometer using the Cu-K$_\alpha$ radiation. The X-ray Laue back-scattering method was utilized to determine the crystal orientation.

3. Experimental results

3.1. Crystallization behaviour and growth parameters of $LiMnPO_4$

Fig. 1 shows the DTA traces of melting and crystallization behaviour of a $LiMnPO_4$ single crystalline specimen in comparison with the single phase powder precursor. The single peak on heating of the single crystalline sample reflects congruent melting of the compound with an onset temperature at 1019 °C. This agrees with microstructure observations in the initial stage of crystal growth where no other primary phase was detected. On cooling the crystallization event arises with a considerable melt undercooling. The wider melting interval of the polycrystalline powder sample does not indicate the inhomogeneous composition only. The lower onset (961 °C) and final temperature also reflect a powder composition with Li excess and Mn depletion (5.7% Li, 31.0% Mn and 61% PO_4 in mass%) determined by ICP-OES analysis, which leads to the reduced melting temperature. This may be compared with the composition of the crystal (4.3% Li, 35.4% Mn and 60.3% PO_4), which is close to the nominal $LiMnPO_4$ stoichiometry (4.4% Li, 35.0% Mn and 60.6% PO_4).

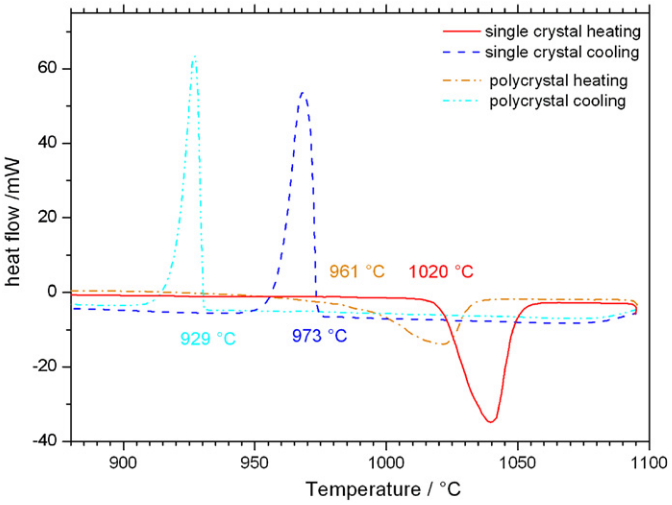

Fig. 1. Isochronal DTA traces on heating and cooling with 20 K/min of a $LiMnPO_4$ single crystal in comparison with the single phase $LiMnPO_4$ powder precursor in Ar atmosphere.

For stable growth of $LiMnPO_4$ the temperature of the floating zone was held between 1100 and 1150 °C, which was determined at the zone surface. A characteristic temperature profile measured by moving the pyrometer vertically along the rod axis from the crystal across the floating zone toward the feed rod is shown in Fig. 2. A sizeable overheating compared to the melting temperature obtained in DTA is necessary for a stable zone and homogeneous melting of the feed rod. However we must bear in mind that in this case the transparency of the melt can eventually lead to a systematic error of the pyrometric measurement. However, from Fig. 2 no appreciable jump in the temperature profile has been detected at the melt/solid phase boundary; therefore we argue that the temperature values are reliable.

Axial temperature gradients $G_{lr} \sim 85 \pm 10$ K/mm on the lower rod at the melt/crystal interface and $G_{ur} \sim 90 \pm 10$ K/mm on the upper rod (melt/feed rod interface) were derived.

A number of floating zone experiments with different growth rates ranging from 1 to 10 mm/h were conducted. The operating temperature is considerably higher than 942 °C (reported for crystal growth of $LiFePO_4$ another potential Li-battery material [4]). This requires elevated Ar gas pressure of 40 bar to prevent vaporization of LiO_2. In Fig. 3 grown crystals from two FZ experiments are visualized. The use of single phase feed rods is an immediate need for the growth of single crystals, which are recognized by their transparency and reddish colour (Fig. 3, bottom). If the feed rod still contains secondary phases ($Li_4Mn_2PO_4$ and $Mn_2P_2O_7$) only a polycrystalline rod was received after the FZ pass, which has an opaque brownish appearance (Fig. 3, top).

Crack formation that occurs shortly after FZ solidification was one serious problem, which deteriorated the perfection of $LiMnPO_4$ crystals. The high temperature gradients and thermal stress during cooling could be a reason. Because of the congruent melting of the $LiMnPO_4$ compound the growth rates could be varied in a wide range between 1 and 10 mm/h with the special intention to avoid (or to reduce) crack formation during the cooling of grown crystals.

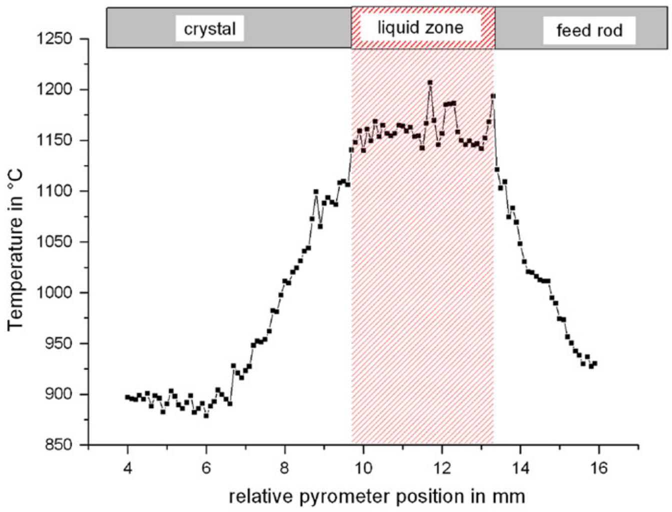

Fig. 2. Axial temperature profile from the crystal across the floating zone toward the feed rod for $LiMnPO_4$ crystal growth.

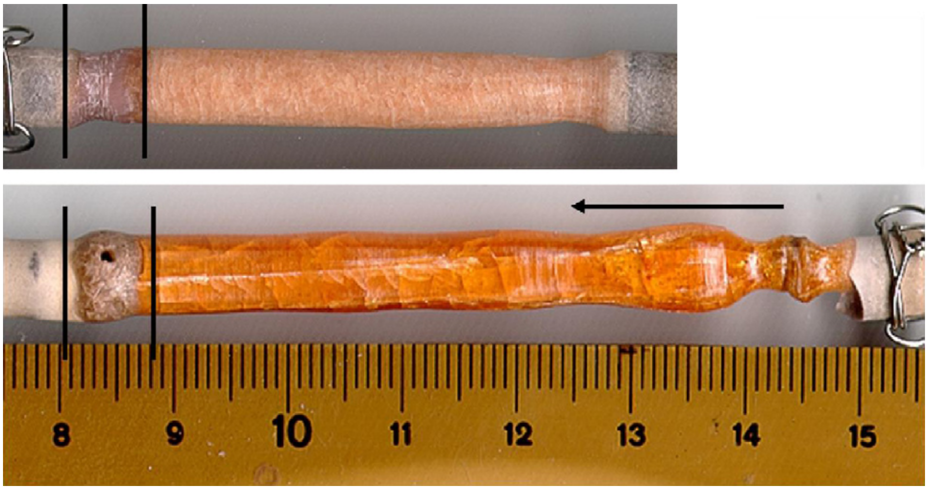

Fig. 3. $LiMnPO_4$ crystal grown with 10 mm/h (bottom) from a single phase feed rod. The growth direction and the quenched last zone (left hand side) are indicated. For comparison a polycrystalline rod (top) received after a FZ pass from a multiphase feed rod is shown.

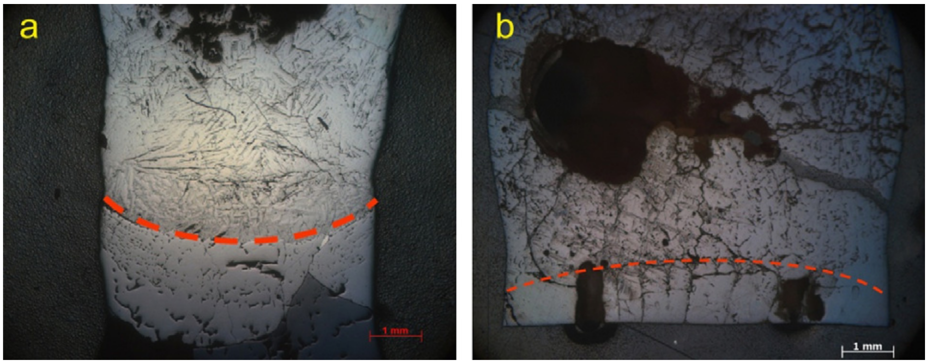

Fig. 4. Polarized light microscopy from the phase border of $LiMnPO_4$ (a) due to the transparency of the liquid zone and light flux above a concave phase border is formed. The grain selection cannot take place. (b) Crystal grown up side down with convex phase border.

Since no effect was achieved and the crystals were of reasonable size, all further experiments were carried out with 10 mm/h to minimize any lithium oxide vaporization.

The crack formation might be solved by applying an after heat treatment during the growth process.

Because of the transparency of the crystal and also because of its illumination through the liquid zone by the vertical light flux from the top, a concave interface between crystal and liquid zone is formed. It can be observed during the growth process and was also proved by a longitudinal section through the rod. The quenched liquid zone is visible on the left hand side in Fig. 4. The concave interface shape disables a proper grain selection, which leads to big columnar grains of 3–4 mm × 2 mm in cross-section and some centimeters in length, which were formed a few millimeters after the start of the growth process. The individual grains on the rod surface point to the single crystalline nature of large parts of the grown rod (cf. Fig. 3).

Due to the asymmetry of the light flux in our vertical growth configuration, the crystallization process depends on the growth direction [12]. Light coming from the top of the upper mirror shines through the transparent liquid, heats up the centre and leads to a concave phase boundary for downward growth of the crystal. For a crystal grown up side down the incident light does not affect the phase boundary. In this case a convex phase boundary was observed.

With proceeding growth process a second phase was detected at the grain boundaries, which eventually stabilizes the grains and prevents a single crystal over the whole cross-section [13]. Towards the end of the growth process the second phase formation in the $LiMnPO_4$ matrix can even deteriorate the growth of big grains. The amount of the minority phase is too small to be analyzed by powder diffraction or chemical analysis methods. However, WDX analyses (without normalization to 100%) provide a rough idea of its composition and hint to a Mn-depleted phase.

Constitutional supercooling and cellular growth can arise at the growth interface because of the composition difference between crystal and floating zone (Fig. 4b). The chemical analysis of the crystal is difficult, because Li is a light element and therefore its content cannot be accurately determined by microprobe analysis neither in the EDX nor in the WDX mode. Chemical analyses (ICP-OES) of a bulk specimen show a deficit of Li and PO_4 in the crystal balanced by excess Mn. On the other hand, in the quenched liquid zone a complementary deficit of Mn and an enrichment of Li and PO_4 ions were detected. During the growth the melt is continuously enriched with PO_4 ions. If a critical concentration difference is exceeded, constitutional supercooling arises. This may explain why the grains are degraded at the end of the growth process.

Although we did not succeed in preparation of perfect centimeter-long single crystalline rods, the coarse grains turned out to be large enough for cutting large single crystalline cuboids of several cubic millimeters in size, which were oriented and utilized for various magnetic measurements and chemical intercalation experiments. The X-ray Laue back-scattering images of large individual grains provide reflections that correspond to the simulated pattern of the orthorhombic Pnma space group and prove the single crystalline nature of the individual grains. The crystallographic structure was further investigated by a four circle diffractometer. The lattice parameters at $T=150$ K of the orthorhombic space group Pnma are (a) 10.419(1) Å, (b) 6.0881(7) Å and (c) 4.7304(5) Å [2].

3.2. *Crystal growth of Li_2CuO_2*

By melting Li_2CuO_2 in air lithium oxide vaporizes. Only by increasing the pressure to 40 bar Ar vaporization can be greatly reduced. The longitudinal section, Fig. 5, illustrates the result of the FZ experiment. No single crystal could be obtained, but the rod consists of a small number of coarse columnar grains (left part of Fig. 4). The typical facets and cleaving planes are missing (cf. top of Fig. 6). The failure of the growth in Ar atmosphere can be explained as follows. During melting, oxygen is released and dissolved in the melt. Obviously oxygen is lost from the FZ because of the low oxygen partial pressure in the growth chamber, and therefore it is not available in the crystallization process. Consequently, copper ions tend to crystallize as Cu^+ ions within a secondary phase $LiCu_2O_2$. The two-phase eutectic crystallization of Li_2CuO_2+ $LiCu_2O_2$ within the grains is visualized in the zoomed part of Fig. 4. The second phase, $LiCu_2O_2$, hinders the grain selection of Li_2CuO_2, as demonstrated in Fig. 5.

By using a gas mixture of Ar:O_2 4:1 at the total pressure of 50 bar, oxygen partial pressure in the growth chamber was increased, which reduced oxygen losses of the melt. The elevated pressure and a growth velocity of 10 mm/h have minimized the vaporization and prevented the crystallization of the secondary phase $LiCu_2O_2$. Nevertheless, evaporation was not completely

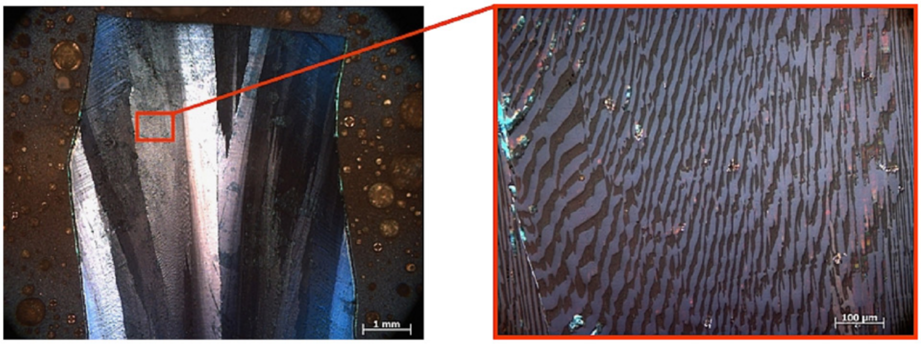

Fig. 5. As-grown Li_2CuO_2 polycrystal in 40 bar argon—secondary phase of $LiCu_2O_2$ (see inset) hinders the grain selection.

Fig. 6. As-grown crystals of Li_2CuO_2 (a) with 40 bar Ar—no single crystal could be obtained and (b) with Ar/O_2 mixture at 50 bar—single crystal, the facets and cleaving planes can be seen.

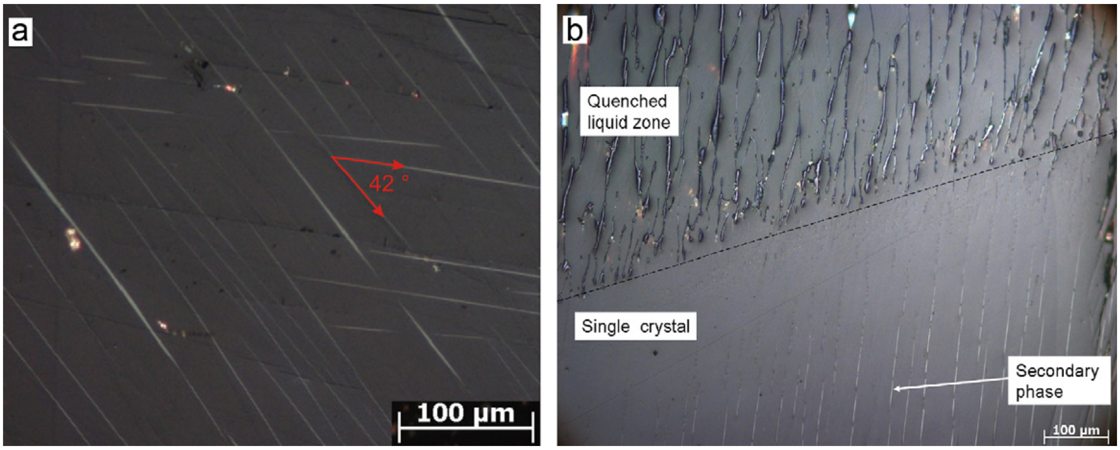

Fig. 7. (a) Optical image of a Li_2CuO_2 crystal showing precipitates of a secondary phase. (b) Optical image in polarized light of a longitudinal section through the crystal (bottom) and the quenched last zone (top), showing the former liquid/solid interface region. The precipitates of a second phase (possibly $LiCu_2O_2$) in the form of well oriented striations in the Li_2CuO_2 crystal matrix are formed a short distance behind the liquid/solid interface.

suppressed. During the growth the lamp power had to be increased because the glass was covered with lithium oxide, which again led to a higher evaporation.

Fig. 6 (bottom) shows an as-grown Li_2CuO_2 crystal. Only after a few millimeters from the start the grain selection is finished that there is only one grain over the complete diameter and facets appear on the surface. In the further growth subgrains can appear in the crystal with tilting angles of 1–7° against each other.

The characteristic growth direction is [0 1 1]. Perpendicular to [1 0 1] Li_2CuO_2 cleaving is very easy, which makes it hard to prepare samples oriented in other directions. Handling of Li_2CuO_2 is difficult because it is very sensitive to humidity and has to be stored in a protective atmosphere.

By analysing the crystals in a polarized light microscope thin striations of precipitates with very definite orientation are detected (Fig. 7). Because the phase occurs only a few millimeters behind the liquid/solid interface (Fig. 7b) it is supposed that it is precipitated in the crystalline matrix because of the retrograde solubility. The nature of the phase could be determined neither by EDX nor by XRD methods because of its small size and volume fraction in the crystal. However because of the observed Li vaporization a lithium-depleted phase, most likely $LiCu_2O_2$, is expected. Attempts to avoid these precipitates by growth with feed rods containing 5% excess Li did not lead to any improvement. However, because of the small volume fraction ($\sim$1%) of this secondary phase no effect on the magnetic or neutron diffraction measurements performed with the crystals [14] were detected.

4. Conclusions

The application of elevated gas pressure turned out to be of crucial importance for single crystal growth of Li-containing compounds, namely $LiMnPO_4$ and Li_2CuO_2, by the Travelling Solvent Floating Zone method. Applying high argon pressure of 40 bar during the growth of $LiMnPO_4$ reduced the vaporization of lithium oxide by orders of magnitude. The conditions were optimized with respect to the growth velocity, 10 mm/h, temperature of the floating zone and the growth direction, which affects the temperature distribution on heating with optical radiation.

The low oxygen partial pressure in the pure Ar atmosphere leads to the loss of oxygen from the molten zone during the crystal growth of Li_2CuO_2 and an undesired change to a two-phase solidification mode. By using an Ar/O_2 gas mixture in the growth chamber the oxygen content in the floating zone is controlled and the solidification of the secondary $LiCu_2O_2$ phase is suppressed. This led to a proper grain selection finally to large Li_2CuO_2 single crystals, which contain only a minor fraction of precipitates in the crystal matrix.

Acknowledgment

The authors would like to thank the BMBF within LIB2015 (Project 03SF0340) for financial support.

References

[1] L. Schramm, G. Behr, W. Löser, K. Wetzig, J. Phase Equilib. Diff. 26 (2005) 605.

[2] N. Wizent, G. Behr, F. Lipps, I. Hellmann, R. Klingeler, V. Kataev, W. Löser, N. Sato, B. Büchner, J. Cryst. Growth 311 (2009) 1273.

[3] P.R. Elliston, J. Phys. Chem. Solids 30 (1969) 1335.

[4] D.P. Chen, A. Maljuk, C.T. Lin, J. Cryst. Growth 284 (2005) 86.

[5] R. Saint-Martin, S. Franger, J. Cryst. Growth 310 (2008) 861.

[6] R. Hoppe, H. Rieck, Z. Anorg. Allg. Chem. 379 (1970) 157 (and references therein).

[7] M. Matsuda, et al., Phys. Rev. B 54 (1996) R15 626.

[8] M. Enderle, et al., Europhys. Lett. 70 (2005) 337.

[9] S.-L. Drechsler, et al., Phys. Rev. Lett. 98 (2007) 07202.

[10] N. Wizent, L. Schramm, G. Behr, W. Löser, W. Gruner, A. Voß, B. Büchner, L. Schultz, J. Solid State Chem. 182 (2009) 2036.

[11] G. Behr, et al., German Patent DE 10 2006 019 807.7 (21.04.2006) and PCT/EP2007/05157 (07.03.2007).

[12] D. Souptel, W. Löser, G. Behr, J. Cryst. Growth 300 (2007) 538.

[13] I. Mazilu, M. Frontzek, W. Löser, G. Behr, A. Teresiak, L. Schultz, J. Cryst. Growth 275 (2005) e103.

[14] W.E.A. Lorenz, R.O. Kuzian, S.-L. Drechsler, W.-D. Stein, N. Wizent, G. Behr, J. Malek, U. Nitzsche, H. Rosner, A. Hiess, W. Schmidt, R. Klingeler, M. Loewenhaupt, B. Büchner, Europhys. Lett. 88 (2009) 37002.